



UHASSELT



Maastricht University

KNOWLEDGE IN ACTION

Faculty of Medicine and Life Sciences
School for Life Sciences

Master of Biomedical Sciences

Master's thesis

Identification of spinal cord injury-induced autoantibodies as prognostic biomarkers using serological antigen selection

Becky Bovens

Thesis presented in fulfillment of the requirements for the degree of Master of Biomedical Sciences, specialization Molecular Mechanisms in Health and Disease

SUPERVISOR :

dr. Judith FRAUSSEN

MENTOR :

Mevrouw Astrid PUES

Transnational University Limburg is a unique collaboration of two universities in two countries: the University of Hasselt and Maastricht University.



UHASSELT

KNOWLEDGE IN ACTION

www.uhasselt.be
Universiteit Hasselt
Campus Hasselt:
Martelarenlaan 42 | 3500 Hasselt
Campus Diepenbeek:
Agoralaan Gebouw D | 3590 Diepenbeek

2020
2021



Maastricht University

Faculty of Medicine and Life Sciences

School for Life Sciences

Master of Biomedical Sciences

Master's thesis

Identification of spinal cord injury-induced autoantibodies as prognostic biomarkers using serological antigen selection

Becky Bovens

Thesis presented in fulfillment of the requirements for the degree of Master of Biomedical Sciences, specialization Molecular Mechanisms in Health and Disease

SUPERVISOR :

dr. Judith FRAUSSEN

MENTOR :

Mevrouw Astrid PUES

Identification of spinal cord injury-induced autoantibodies as prognostic biomarkers using serological antigen selection*Becky Bovens¹, Astrid Pues¹, Patrick Vandormael¹, Veerle Somers¹ and Judith Fraussen¹¹ Department of Immunology and Infection, Biomedical Research Institute, Hasselt University, Martelarenlaan 42, 3500 Hasselt, Belgium*Running title: *Spinal cord injury-induced autoantibodies*

To whom correspondence should be addressed: Judith Fraussen, Tel: +3211269270; Email: judith.fraussen@uhasselt.be

Keywords: Autoantibodies, Serological Antigen Selection, Spinal cord injury, Biomarker-based prediction, cDNA phage display library**ABSTRACT**

BACKGROUND: Spinal cord injury (SCI) is a devastating condition, leading to sensory and motor function loss. SCI disrupts the blood-spinal cord barrier, releasing SCI-related proteins in the blood stream, triggering autoimmune responses and the production of autoantibodies. Since there are no predictive strategies for the SCI-outcome, these SCI-induced autoantibodies can be valuable as prognostic disease markers, especially in patients with worsening of the SCI. Our aim was to identify a full spectrum of SCI-induced autoantibodies from SCI patients' plasma using serological antigen selection (SAS).

METHODS: To assess SCI-induction of the autoantibodies and the samples' suitability for the SAS, immunoglobulin (Ig)M and IgG levels in SCI patients' plasma were determined 0-4 days post injury (DPI) and 20-33 DPI using ELISA. Next, IgM ELISA and SAS procedures were optimised. SAS used a cDNA phage display library expressing spinal cord proteins, which was screened for SCI-induced autoantibody reactivity using pooled plasma of 12 SCI patients with known worsening of the SCI. Phage expressing antigens to which SCI-induced autoantibodies bound were selected. Selected antigenic targets were characterised using colony PCR and DNA fingerprinting.

RESULTS: SCI patients' total plasma IgM levels were significantly increased ($p=0.0491$) 20-33 DPI compared to 0-4 DPI, in contrast, IgG levels remained stable ($p=0.3474$). SAS and phage ELISA data suggested an increased selection of phage expressing antigens with SCI-induced autoantibody reactivity. DNA fingerprinting of the selected clones identified

five digestion patterns, confirming enrichment of phage.

CONCLUSION: After successful optimisation, SAS could identify SCI-induced autoantibodies with prognostic biomarker potential.

INTRODUCTION

Spinal cord injury (SCI) is a devastating condition, leading to temporary or permanent sensory and motor function loss (1). Paralysis of voluntary muscles and loss of sensation reduces SCI patients' mobility and functional independence, negatively affecting their health and well-being (2, 3). Globally, there are between 250,000 to 500,000 new SCI cases every year (4). The majority of these new cases are traumatic SCI caused by road traffic accidents, falls, sports or recreational injuries and other causes (4). Currently, SCI is diagnosed and classified by imaging of the lesion using magnetic resonance imaging (MRI), which provides information about the lesion size, location and haemorrhage (5). Neurological examination using the American Spinal Injury Association (ASIA) impairment scale (AIS) is performed to define the sensory and motor impairment post-injury (5-7). This scale classifies the patients into five groups: A, B, C, D and E. Patients in group A have a complete SCI with no preserved sensory or motor function, whereas groups B-D have increasing function, and group E has a normal function (7). SCI treatment focusses on neuroprotection, physical therapy, anti-inflammation and surgical decompression (8, 9).

During a SCI, the spinal cord is damaged, primarily caused by damaged neurons and axons in the lesion area. SCI also disrupts the blood-spinal cord barrier, releasing proteins from the

central nervous system (CNS) into the bloodstream (10). The released proteins can be structural or functional and are derived from damaged connective and nervous tissue. Within hours, innate immune cells such as neutrophils, macrophages, and dendritic cells arrive at the site of injury and begin clearing debris while recruiting other inflammatory cells (11). Naive B cells residing in the lymph nodes recognise the CNS antigens in the blood stream and become activated. The activated B cells start to proliferate, differentiate into plasma cells, and migrate to the lesion site. After differentiation, the B cells produce cytokines and antibodies (12). Hence, five to ten days post-injury, plasma cells secrete immunoglobulin (Ig) M autoantibodies. Later, around day 20 to 25 post-injury, the plasma cells secrete IgG after undergoing isotype switching and affinity maturation (13). B cells and plasma cells accumulate in the spinal cord, producing high levels of SCI-induced autoantibodies (14-16). The production of both cytokines and antibodies induces a neuroinflammatory state, possibly leading to an increased SCI lesion (14). The corresponding additional neuronal and axonal damage often leads to secondary chronic complications such as neuropathic pain, cardiovascular or respiratory complications and possible spasticity (1, 15).

To exert their effector functions antibodies bind to receptors or directly to antigens, activating or deactivating pathways (17, 18). Furthermore, IgG can coat antigens and bind Fc γ -receptors, stimulating phagocytosis or antibody-dependent cellular cytotoxicity (ADCC) (14, 17, 19, 20). Moreover, both IgM and IgG are able to interact with the complement protein C1, activating the classical pathway of the complement system (14, 21).

Previous research in mice has established B cell accumulation with subsequently elevated IgM and IgG levels in SCI lesions (14-16). These SCI-induced autoantibodies are found to have pathogenic and neuroinflammatory effects in mice (14, 15). Passive transfer of these antibodies into uninjured wild type mice induced neuroinflammation and degeneration of the spinal cord tissue (14). The neuropathology was caused by antibodies activating the complement system and cells expressing Fc γ -receptors such as phagocytes (14, 19, 22).

The diagnosis of SCI is often indisputable, the prognosis of the SCI course is not. Differences in injury pattern, severity, location, pre-injury health situation, and genetic background result in

an extensively heterogeneous SCI patient population, complicating the SCI course prediction (23). Therefore, there is a necessity for novel, accessible, reliable, and objective methods to predict the course of SCI, such as the use of biomarkers (24). Autoantibodies have proven to be promising biomarkers in multiple autoimmune diseases (25, 26). Accordingly, our research group has previously identified autoantibodies as potential biomarkers in rheumatoid arthritis and multiple sclerosis (25, 26). However, knowledge of SCI-induced autoantibodies is still limited.

Previous research has established increased antibody responses to several CNS-derived proteins in SCI patients (27-30). These studies have correlated elevated antibody titres to structural CNS proteins, such as neurofilament light chain (NF-L), glial fibrillary acidic protein (GFAP), myelin basic protein (MBP) and neuron-specific enolase (NSE), with injury severity (27-29). Elevated antibody levels in the serum against NF-L were even associated with poorer neurological prognosis (27). Nonetheless, much of the research has been performed on animal samples, reducing the translatability to the human situation or on human cerebrospinal fluid (CSF), which is more invasive to obtain (31). Furthermore, the sample size of these studies was limited. Consequently, there is still a need for an elaborate identification of the full spectrum of SCI-induced autoantibody responses and their correlation with SCI prognosis.

Selecting and identifying the full spectrum of SCI-induced autoantibodies can provide clinically relevant biomarkers for SCI prognosis. Therefore, we will use serological antigen selection (SAS). SAS is an innovative high-throughput method based on complementary DNA (cDNA) phage display for the selection of an extensive range of antigenic targets (26, 32). In this study, a cDNA phage display library constructed from human spinal cord tissue was used, providing a tissue-specific expression system to study SCI. This library consists of filamentous M13-phage containing phagemids with cDNA fragments fused to the gene for coat protein VI (25). As a result, the phage express spinal cord proteins or peptides on their surface (25). The phage library is then incubated with antibodies from SCI patients' plasma samples. The SCI-induced autoantibodies in the plasma will interact with their specific antigens creating high-affinity complexes (24, 32). As this process is repeated for multiple selection rounds, only the highest affinity antibody-antigen interactions will

be selected and the antigens are identified. Besides the identification of known proteins, SAS also allows the selection and identification of novel uncharacterised proteins (24, 32).

Our aim is to identify a broad array of SCI-induced IgM and IgG autoantibodies from the plasma of SCI patients. We aim to observe the SCI-induced autoantibody responses at 0-4 days post injury (DPI) and 20-33 DPI, while optimising techniques such as an in-house IgM ELISA and IgM SAS. Furthermore, using the patients' autoantibody repertoire to identify antigenic targets using a cDNA phage display library constructed from human spinal cord tissue and subsequently selection using IgG SAS. Gaining insight about the humoral responses after SCI could lead to the identification of promising autoantibody biomarker candidates.

EXPERIMENTAL PROCEDURES

Plasma samples used in this study – Plasma samples were obtained from traumatic SCI patients in University Hospital Leuven (Leuven, Belgium), Hospital East-Limburg (Genk, Belgium), Jessa Hospital (Hasselt, Belgium), Adelante Rehabilitation Centre (Hoensbroek, The Netherlands), Neurosurgery Maastricht (Maastricht, The Netherlands) and the University of Queensland (Brisbane, Australia) via the University Biobank Limburg (UBiLim). The samples were collected at two time points, at 1-4 DPI (T0) and 20-33 DPI (T1). Additional personal information of the patients, such as age, gender, AIS classes, motor and sensory scores, time and cause of injury, treatment, and the exact time of sample collection, was acquired (Table 1). Written informed consent was collected from all participants. Approval of the local Ethical Committee has been obtained for the collection and use of the patient samples. Patients with pre-existing autoimmune disorders or who received anti-inflammatory treatment were excluded from the study. Patients with AIS scores A, B or C that showed no improvement of the SCI and had both

a T0 and a T1 sample were included. A total of 12 SCI patients and 15 healthy controls (HC) were involved in this study. Plasma samples of HC were used for optimising the IgM ELISA and the IgM SAS. Plasma samples from HC were also obtained via UBiLim. For the SAS, 20µl plasma per patient was pooled (diluted 1/100) to make the T0 and the T1 pools. The T0 pool, which contained baseline autoantibodies that had not been SCI-induced, was used for the SAS's negative selection, whereas the SCI-induced autoantibodies in the T1 pool were used for positive selection. Similarly, 20µl plasma of the HC was pooled (diluted 1/100) for the HC pool.

Phage production and precipitation – To produce phage, *Escherichia coli* (*E. coli*) TG1 cells were grown to an optical density (OD) of 0.5 in 10% glucose (Millipore, Leuven, Belgium, 1.08337.1000) 1µg/ml ampicillin 2x yeast extract tryptone (GA-2xYT) (Difco 2xYT, BD, Erembodegem, Belgium, 244020) medium. The cDNA display library constructed from healthy spinal cord tissue as described previously, was thawed from the stock and added to the TG1 bacteria with helper phage for infection (10, 24). As will be discussed further on, some SAS conditions were produced with 100µM isopropyl thio-b-D-galactopyranoside (IPTG, Invitrogen, Geel, Belgium, 15529-019) added. IPTG activates the *Lac* promotor and hereby increases the expression of fusion proteins in phage (33, 34). The infection mixture was incubated in a water bath at 37°C for 30 minutes. After which it was centrifuged for ten minutes at 2800g. The supernatant was discarded and the pellet resuspended in ampicillin kanamycin 2xYT medium and grown overnight at 30°C while shaking. The next day, the bacteria were centrifuged for 20 minutes at 4°C at 3500g. To the supernatant polyethylene glycol sodium chloride (PEG-NaCl) was added and incubated on ice for one hour, to precipitate the phage. Then centrifuged again for 15 minutes at 4°C at 3500g. The supernatant was discarded and the pellet was

Table 1 – Summary of SCI patients characteristics included in this study.

	Age	Gender		AIS Class			Injury level	
		Male	Female	A	B	C	Cervical	Thoracic
SCI	47 ± 22.9 years	11 (91.7%)	1 (8.3%)	8 (66.7%)	3 (25%)	1 (8.3%)	7 (58.3%)	5 (41.7%)

Data are presented as mean ± standard deviation or number of patients with percentage. With SCI, spinal cord injury and AIS, American spinal injury association impairment scale.

dissolved in sterile 1x phosphate-buffered saline (PBS) after which it was centrifuged for two minutes at 4°C at 13000g. PEG-NaCl was again added and incubated on ice for 15 minutes. Then it was centrifuged again for five minutes at 4°C at 13000g after which the pellet was resuspended in 1x PBS. One more centrifugation step of two minutes at 4°C at 13000g was done after which the phage in the supernatant were precipitated and purified.

Serological antigen selection procedure – SAS was performed to identify enriched phage clones using the spinal cord library, containing 2.44×10^6 independent (10, 24). First, antibodies reactive to M13 phage and *E. coli* protein extracts were removed from the patients' plasma by preadsorption using Cyanogen bromide-activated-Sepharose 4B beads (Sigma-Aldrich, Overijse, Belgium, C9142-5G) coated with these extracts. To form two phage and two bacterial columns, 0.25g beads were coupled with 2500µg of phage and bacterial extracts, respectively. The bacterial columns were washed with 1x tris-buffered saline (TBS) and incubated with the pooled plasma of 12 SCI patients overnight at 4°C while rotating. Next, the bacterial column was centrifuged for five minutes and the supernatant was added to the phage column and again incubated overnight. The phage column was then centrifuged for five minutes at 500g, and the supernatant, depleted from antibodies reactive to phage and bacterial proteins, was used for the IgG SAS.

The preadsorbed plasma was then depleted from IgM by incubation with IgM beads (Anti-Human IgM µ-chain specific-Agarose beads, Sigma-Aldrich, Overijse, Belgium, A9935) for 60 minutes.

Four different SAS conditions were tested: in condition A, pooled SCI plasma was incubated with the phage display library, condition B was a negative control of condition A, incubated with PBS instead of plasma, to observe non-specific phage plaque. In condition C the same pooled plasma as condition A was used, but it was incubated with phage from the library produced with IPTG, while D served as a negative control of condition C with no plasma. Four consecutive SAS rounds were performed. The first round consisted of one negative and one positive selection. The next three rounds consisted of two negative selections and a positive selection. During the negative selection, pooled T0 samples were preincubated with the phage of the SCI library for 60 minutes at room temperature (RT)

while rotating. During the preincubation, antibodies from the plasma specific for particular antigens displayed by phage formed antibody-phage complexes. Meanwhile, 200µl Protein G Resin selection beads (GenScript, Huissen, The Netherlands, L00209) were incubated with a blocking mixture consisting of 2% MPBS, 100µg/ml phage extract and 1x PBS for 60 minutes while rotating. The preincubation mixture was then added to the blocked beads and incubated for ten minutes at RT while rotating. After incubation, the mixture was centrifuged for five seconds, and the supernatant, depleted from phage bound by antibodies of the T0 sample, was used as the input for the second negative selection. Positive selection was then performed using the supernatant of the second negative selection. The pooled T1 samples were incubated with the supernatant for 60 minutes at RT while rotating. The preincubation mixture was added to the blocked beads and incubated for 30 minutes at RT while rotating. After incubation, the positive selection mixture was centrifuged for five seconds, and the beads were washed ten times with PBS with 0.01% Tween20 (0.01% PBS-T, Sigma-Aldrich, Overijse, Belgium) and five times with 1x PBS to remove unbound phage. The bound phage-antibody complexes were eluted with 100mM triethylamine (TEA, pH 12) for ten minutes and then with 100mM glycine (pH 2.5) for ten minutes. The elutions were neutralised using 1M tris-HCl (pH 7.4).

Each round's input and output were amplified and titrated by infecting *E. coli* TG1 bacteria and plating them on small GA-2xYT agar (Bacto-agar, BD, Erembodegem, Belgium, 214010) plates. Furthermore, the outputs were amplified and plated on large GA-2xYT plates as input for subsequent SAS rounds.

Colony polymerase chain reaction, DNA fingerprinting and enzymatical digest – To identify the enriched phage clones, single colonies were picked from the titration plates of the fourth SAS round and inserted into U bottom 96-well plates (Greiner, Bio-one, Wommel, Belgium, 650180) filled with GA-2xYT medium and grown overnight at RT. To 2µl of the liquid culture, 58µl of polymerase chain reaction (PCR) master mix (nuclease-free water, 10X PCR reaction buffer with MgCl₂, 20mM dNTPs, 10µM PV289 Forward oligo [Integrated DNA technologies, Leuven], 10µM PV219 Reverse oligo [Integrated DNA technologies, Leuven], 10% Taq DNA Polymerase) was added. The

primers used were listed in **Table 2**. The reactions

Primers	Sequence (5' to 3')
PV289	TCCCCGAAGCCATTCTATC
PV219	ACAGACGTTCCGCTAATTC

were then placed in the thermal cycler for a cycle consisting of ten minutes at 94°C, to release the DNA from the bacteria, followed by 30 cycles of DNA denaturation at 94°C for 20 seconds, 30 seconds for primers to anneal at 58°C, and extension at 68°C for three minutes, with a final extension step at 68°C for five minutes. The PCR products were visualised by gel electrophoresis on 1% agarose gels using a SmartLadder (Eurogentec, Seraing, Belgium, MW-1700-10). Next, the PCR products were enzymatically digested using BstNI (NEB, Leiden, The Netherlands, nuclease free water, buffer Neb 3.1 and BstNI) at 60°C and CviQI (NEB, Leiden, The Netherlands, nuclease free water, buffer Neb 3.1 and CviQI) at 25°C for three hours, and analysed on 1% agarose gels.

Statistical analysis – Data were analysed using Microsoft EXCEL and GraphPad Prism 9 for Windows (GraphPad Software, San Diego, USA). Normality was tested using the Shapiro-Wilk test and QQ-plots. The Grubbs' test was used to test for outliers. To compare two groups, student T-tests were performed if data were normally distributed and otherwise the non-parametric Mann-Whitney test was utilised. A two-sided p-value of <0.05 was considered statistically significant. Additional extensive experimental procedures can be found in the **Supplementals** section.

RESULTS

Patient characteristics – The 12 selected SCI patients, including 11 males and one female, had a mean age of 47 ± 22.9 years old (**Table 1**). Based on neurological examination, the majority of the patients was classified with AIS A (66.7%), a quarter of the patients with AIS B (25%), and only one patient with AIS C (8.3%). In addition, seven out of the 12 patients had a cervical injury, whereas five were injured at the thoracic level.

IgM ELISA optimisation – To optimise the IgM ELISA protocol, different concentrations for the IgM coating antibody, either 1µg/ml or 10µg/ml, were tested. The 1µg/ml ($R^2=0.9926$) concentration was the most promising compared

to the 10µg/ml ($R^2=0.8081$) concentration (data not shown). Variations on the IgM standard dilutions were tested, of which six 1:2 dilutions starting from 100ng/ml were optimal. Additionally, two detection antibodies, rabbit anti-human IgM-HRP (Sigma-Aldrich) and rabbit anti-human IgM-HRP (Jackson, Zottegem, Belgium, 109-036-129), were tested, after which the Sigma antibody ($R^2=0.9917$) was preferred over the Jackson antibody ($R^2=0.9880$, data not shown), and the in-house IgM ELISA was optimised.

Total IgM levels increased 20-33 days post-SCI, but IgG levels did not – To gain insight into the overall antibody responses after SCI and determine the suitability of the patient samples for the SAS, total IgM and IgG concentrations were measured from SCI patients' plasma using IgM and IgG ELISA. Total plasma levels of IgM in SCI patients were significantly increased at 20-33 DPI (T1) compared to baseline levels (T0) ($p=0.0491$) (**Figure 1B**). Nine of the 12 patients showed increased IgM levels at T1, two of them showed difference in IgM levels between the 2 time points, and one patient had a slight decline in IgM levels over time (**Figure 1A**). When comparing patients with a cervical and thoracic injury there was a significant increase in IgM levels for the thoracic group ($p=0.0317$), but not for the cervical group ($p=0.4021$) (**Supplementary figure 1A-B**). Furthermore, there was no difference in IgM levels at 20-33 DPI between thoracic and cervical SCI patients (**Supplementary figure 1E**). Additionally, there were no variations in IgM levels at T1 when comparing IgM levels based on AIS class (A, B, and C) ($p=0.2379$, data not shown).

The SCI patients' IgG levels, remained stable comparing baseline (T0) and 20-33 DPI (T1) ($p=0.3474$) (**Figure 1D**). Eight of the 12 patients had increased IgG levels and four a decrease in IgG (**Figure 1C**). Similar to the IgM levels, there were no differences in IgG concentration T0-T1 in the cervical group ($p>0.9999$) and the thoracic ($p=0.3095$) (**Supplementary figure 1C-D**). Moreover, comparing IgG levels at T1 between thoracic and cervical level did not lead to a significant difference (**Supplementary figure 1F**). AIS class did not affect IgG levels at T1 ($p=0.8505$, data not shown). Altogether, after optimising the in-house IgM ELISA, the IgM and IgG levels were determined of the 12 SCI patients. IgM levels were increased 20-33 DPI compared to baseline levels, whereas IgG remained stable. In order to

use the T0 samples for negative selection and the T1 samples for positive selection in the SAS, the T0 samples had to be lower in IgM and IgG than the T1 samples. Therefore, since nine patients had elevated IgM levels and eight patients had elevated IgG levels at T1, the samples could be used for the SAS.

Optimisation of the SAS protocol utilising IgM beads – Beads are used to bind the high affinity antibody-antigen complexes produced during the SAS selection. Antibodies bind to the beads, selecting the attached phage while washing away the unbound beads. Whereas the IgG selection beads had been used before, the IgM beads were new and untested by our research group. For the optimisation, plasma samples of 15

HC with IgM concentrations similar to the SCI patients were selected and their plasma was pooled (**Supplementary table 1**). The IgM beads were incubated with the pooled plasma for zero, ten, 30 or 60 minutes. For each incubation, the supernatant was used to compare the beads' binding capacity and cross-reactivity to IgG by measuring the IgM and IgG concentration with ELISA. The IgM concentration of the plasma pool before incubation was considered as 100% or as 0% IgM bound by the beads (Input), the concentration IgM in the supernatant at the different incubation times (T0, T10, T30 and T60) and the elutions were compared to this input as percentage bound to the IgM selection beads.

In the first test, IgM was eluted from the beads using TEA and glycine. The first test showed that after 60 minutes, the majority of IgM (97.42%) was bound to the beads, however, after elution with TEA only 11.91% of the IgM was eluted and a second elution with glycine resulted in no additional IgM (**Supplementary table 2**). The cross-reactivity of the IgM beads to IgG was tested by performing IgG ELISA and showed that up to 20% of the IgG in the sample bound to the IgM beads (**Supplementary table 3**).

To increase the fraction of eluted IgM, the elution steps were switched in the second test, the beads were eluted with glycine first and then with TEA. Furthermore, to reduce the cross-reactivity towards IgG, the plasma used for the second IgM beads test was first depleted of IgG using IgG selection beads. As a result, the second test showed a lower binding capacity after 60 minutes of 76.34% and the elution was not elevated by this change (**Supplementary table 2**). However, test 2 showed that the predepletion of IgG was successful and removed 100% of all IgG in the sample (**Supplementary table 3**). Unfortunately, this predepletion step also removed 25% of the IgM from the sample (data not shown).

A third test was performed to test if the decreased binding capacity observed in test 2 was due to the predepletion of IgG, and to confirm the results of the predepletion in test 2. The third test contained an IgG predepletion step but was only eluted with TEA. The IgM binding capacity after 60 minutes was 92.78% and the elution went up to 20.10%, confirming the predepletion did not affect the binding capacity (**Supplementary table 2**). However, still 20% of the IgM in the sample was lost.

Therefore, a fourth test was performed to determine if blocking the IgG predepletion beads with IgM standard would be useful in decreasing

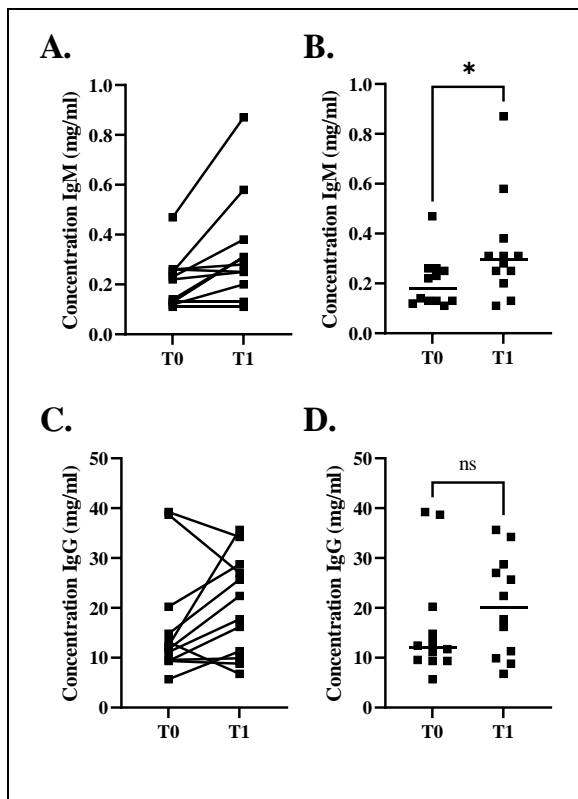


Figure 1 – Total IgM and IgG levels in the plasma of SCI patients at two timepoints as measured by IgM and IgG ELISA. A-B. IgM plasma concentration of 15 SCI patients at T0 and T1. **C-D.** IgG plasma concentration of SCI patients at T0 and T1. With IgM, immunoglobulin M; IgG, immunoglobulin G; T0, plasma samples collected one to four days post injury; T1, 20-33 days post injury; ns, not significant. The horizontal line on the figures represents the median of the data. All data were tested with a non-parametric Mann-Whitney test. (n=12) *p<0.05.

their cross-reactivity towards IgM and counteracting this loss of IgM, but it was unsuccessful (data not shown).

Serological antigen selection with IgG using the spinal cord cDNA display library – SAS was used to identify SCI-induced antibodies and their antigenic targets. Four consecutive selection rounds were performed using the spinal cord cDNA phage display library and the pooled plasma of 12 SCI patients. T0 samples, which contained baseline antibodies that had not been induced by SCI, were utilised for negative selection, while T1 samples were utilised for positive selection. As previously stated, we tested four different conditions, with condition A being SCI plasma incubated with the phage of the spinal cord library, whereas condition B is the negative control of A in which the library was incubated with PBS. Condition C consisted of phage produced while stimulated by IPTG and incubated with plasma and condition D was the negative control of C.

In the first round, all conditions started with input phage titres ranging from 1.13 to 2.35×10^{13} colony forming units (cfu) (**Supplementary table 4**). After the first negative selection, these titres were decreased slightly to $2.65 - 6.5 \times 10^{12}$ cfu due to the removal of non-specific phage. The first output after TEA elution and the second output after glycine elution did not differ between conditions, with titres ranging from 1.05 to 2.39×10^7 cfu. The outputs of the conditions with plasma, A (1.60×10^7 cfu) and C (1.10×10^7 cfu), did not appear to be different from their negative controls, B (1.11×10^7 cfu) and D (1.07×10^7 cfu). Furthermore, the phage titres of conditions with phage produced without IPTG, A and B, did not differ from those with IPTG, C and D. All conditions had comparable ratios (third input/first output: A, 4.08×10^5 ; B, 2.40×10^5 ; C, 2.54×10^5 and D, 5.89×10^5).

The second round consisted of two negative selections and a positive selection of all the conditions. The input of the A condition (4.15×10^{12} cfu) was reduced in contrast to the other conditions ($1.07 - 9.70 \times 10^{13}$ cfu). However, A's output (6.20×10^6 cfu) was similar to the outputs of the other conditions ($2.34 - 5.45 \times 10^6$ cfu). Comparing the ratios of condition A (6.47×10^5 cfu) and its negative control B (4.25×10^6 cfu), A had lower ratios, implying more phage enrichment than B. Similarly, the ratios of condition C (2.46×10^6 cfu) were ten times lower than D (2.39×10^7 cfu). Despite these minor differences, the ratios were increased compared

to the first selection round. Enrichment implies that specific phage clones have become amplified over the SAS rounds. Phage to which SCI-induced antibodies are reactive to will become selected and amplified each round, increasing the output, while the input stays the same, decreasing the ratios.

In the third round, an additional novel negative condition of A was added, condition A*, this condition started from the same input as condition A in round three (and four). This condition was added to observe non-specific phage plaque and to compare to condition A. Furthermore, A* was a novel negative control of A in which non-specific phage had not been enriched for three rounds, as was the case in condition B. Input titres were very similar for all conditions ($3 - 5.80 \times 10^{13}$ cfu). Although the output of condition A (8.75×10^7 cfu) was double the output of condition B (4.85×10^7 cfu), A*'s output (7.30×10^7 cfu) was comparable to A. In the outputs of C (8.11×10^7 cfu) and D (3.66×10^7 cfu) the same difference was observed. The ratios of the conditions incubated with plasma, A (5.58×10^5 cfu) and C (1.39×10^5 cfu), were slightly lower than those without plasma, B (8.83×10^5 cfu) and D (9.61×10^5 cfu), however, this was not the case for A* (5.29×10^5 cfu). The ratios were decreased when compared to the second round, implying phage enrichment.

Lastly, the fourth round also included an A* condition starting from the input of A. Moreover, after the elution of the positive selection of this round, an additional negative selection without using T0 plasma was performed to reduce the amount of non-specific phage for conditions A, B and A*. The inputs of the conditions again were very similar ($1.94 - 4.80 \times 10^{13}$ cfu), but condition C (3.68×10^7 cfu) and A* (4.93×10^7 cfu) had higher outputs than conditions A (1.65×10^6 cfu), B (4.74×10^6 cfu) and D (3.42×10^6 cfu). Therefore, C (1.75×10^5 cfu) and A*'s ratios (3.46×10^5 cfu) were decreased compared to A (9.44×10^6 cfu), B (6.65×10^6 cfu) and D (2.05×10^6). The additional negative selection of A, A* and B started with inputs of 5.05×10^5 cfu (A), 2.19×10^6 cfu (A*) and 9.23×10^5 cfu (B). The output of A* (1.40×10^5 cfu) and B (1.43×10^5 cfu) were a little elevated compared to A (6.76×10^4 cfu), but the ratios (input 4/output 3) of A (7.47×10^0 cfu) and B (6.44×10^0 cfu) were lower than the A* (1.57×10^1 cfu) condition. Nevertheless, when comparing the ratios of the fourth round to the third round, the fourth round did not show more enrichment than the third

round. Eventually, based on the output titres and ratios, there did not appear to be any difference in the enrichment of the conditions across the four rounds of SAS. The outputs of the fourth round of SAS were DNA fingerprinted.

DNA fingerprinting of selected cDNA inserts reveals five recurring patterns – To identify enriched cDNA clones selected by SAS, a total of 2016 individual colonies from the output of the fourth SAS round were randomly selected. The cDNA inserts of 192 of them, 96 of condition A and 96 of condition B, were amplified using colony PCR and enzymatically digested by BstNI and CviQI. Examples of restriction enzyme digests with BstNI and CviQI are shown in the gels depicted in **Figure 2**. Additionally, **Table 3** provides an overview of the colony PCR and enzymatic digests with BstNI and CviQI. Colony PCR was successful in 66.67% of the cases. Amplification of the cDNA inserts resulted in fragments ranging from two to 1000 base pairs (bp). Enzymatic digests with BstNI and CviQI identified five different digestion patterns, 1, 2, 3, 4 and 5 (**Figure 2** and **Table 3**). Patterns 1-4 were discovered in the selected colonies of both conditions A and B. In contrast, pattern 5 was not observed in condition B. The total number of inserts with a pattern in condition A was 33 colonies, compared to 32 colonies in condition B. Furthermore, the ratio of patterns was higher in condition A (53.23%) than in B (48.48%), indicating that condition A was more enriched than condition B.

Phage ELISA shows enrichment across four rounds of SAS – To determine phage enrichment SCI autoantibody reactivity was tested against phage of the in- and output samples from all SAS rounds for each condition. Enrichment of specific phage would result in increased reactivity over the consecutive SAS rounds. To determine the reactivity to the specific displayed antigens, the ratio of reactivity towards SAS phage to empty phage was calculated. Furthermore, to investigate the effect of positive and negative selection in the SAS, the reactivity of both T0 and T1 sample pools was tested against the same phage in- and outputs.

Conditions A, A*, and B started with the same input, the spinal cord library produced without IPTG, while conditions C and D began with the spinal cord library produced with IPTG. After the first round the reactivity decreased slightly in all conditions except C (**Figure 3**). Right from the start, there was a small difference when comparing antibody reactivity at baseline

(T0) to 20-33 DPI (T1), T1 was increased (**Figure 3**). Over the next two rounds, the reactivity of T1 samples in conditions A and C increased from 1.266 (Round 2 IN) to 2.580 (Round 4 IN) and from 1.399 to 3.129, respectively, with a noticeable difference in reactivity between T0 and T1 samples (**Figure 3A and C**). Moreover, when condition A was compared to its negative control B (Round 4 IN), B's reactivity (1.115) was lower than A's (2.580) (**Figure 3A-B**). Similar, D (1.189) was also decreased compared to C (3.129) (**Figure 3C-D**).

For the fourth round's output, however, reactivity decreased for conditions A (2.227) and C (2.769), while B (1.388) and D (1.245) remained constant and A* strongly increased from 2.580 to 4.755. Over the four rounds of SAS, a noticeable increase in reactivity, and thus enrichment, was observed in conditions A (1.479-2.227) and C. (1.381-2.769), whereas their negative controls, B (1.479-1.388) and D (1.381-1.245), remained stable (**Figure 3**). Whereas condition A's reactivity was increased by 1.5 times, condition C's reactivity increased two-fold over the course of four rounds. Furthermore, the reactivity of the T1 antibodies was higher than that of the T0 antibodies, indicating that the SAS showed enrichment.

DISCUSSION

In this study, the aim was to explore a broad array of SCI-induced autoantibodies from the plasma of SCI patients using SAS. First, we optimised the IgM ELISA and characterised the patient plasma samples using IgM and IgG ELISA. Furthermore, we optimised the use of IgM selection beads for the SAS using pooled plasma of 15 HC. After optimisation, the IgG SAS was performed using pooled plasma of 12 SCI patients with known worsening of the SCI in combination with a human spinal cord phage display library. The SAS and the spinal cord phage display library provided us with a disease-relevant system to study the antibody responses in SCI. Selected antigenic targets of SCI-induced autoantibodies were identified using colony PCR and DNA fingerprinting with enzymatic digestion by BstNI and CviQI.

After optimisation of the IgM ELISA, total IgM and IgG plasma levels were determined to observe the antibody responses post SCI and to determine if the T0 and T1 samples could be used for the SAS. The T0 samples had to be lower in IgM and IgG than the T1 samples in order for

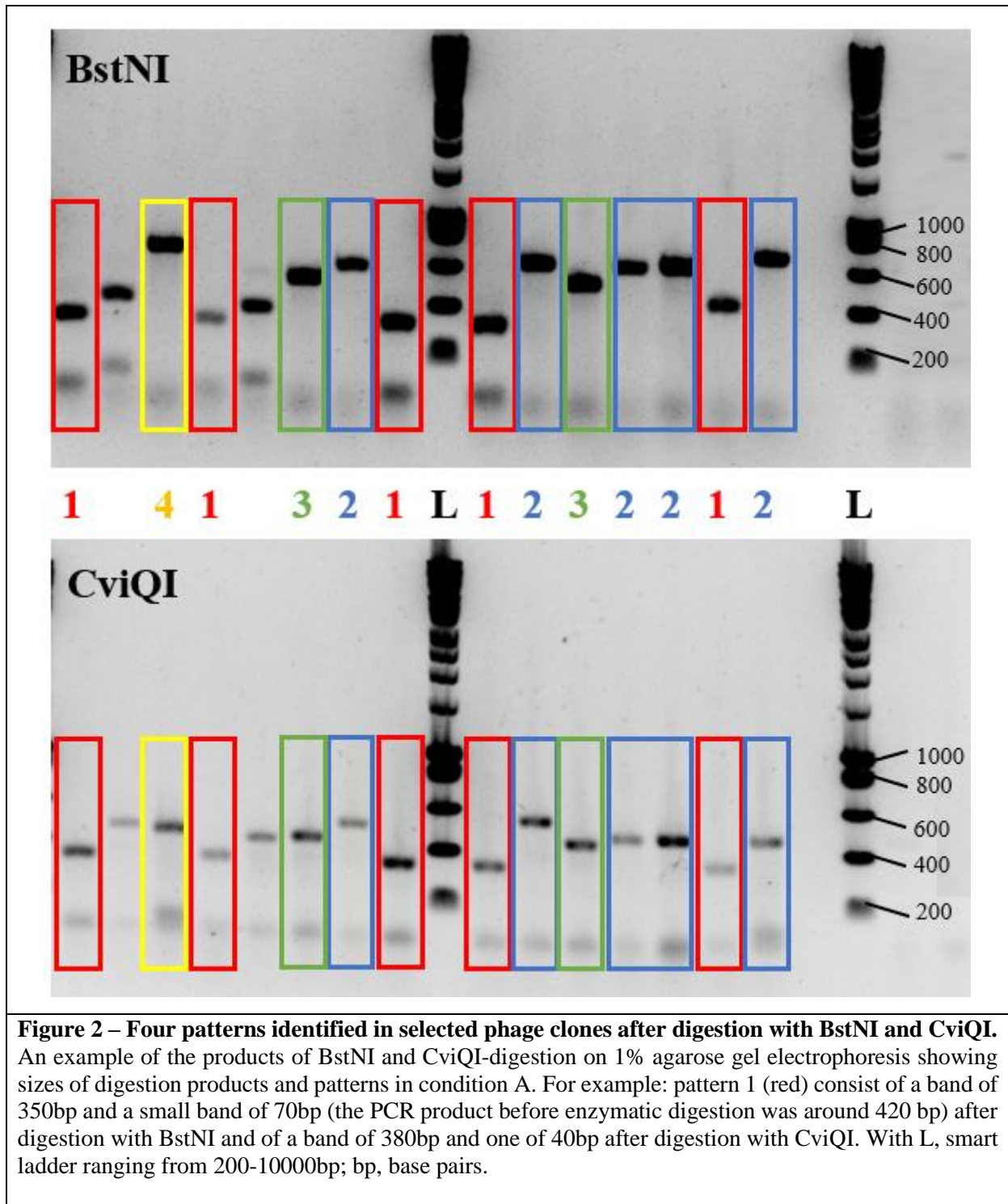


Figure 2 – Four patterns identified in selected phage clones after digestion with BstNI and CviQI. An example of the products of BstNI and CviQI-digestion on 1% agarose gel electrophoresis showing sizes of digestion products and patterns in condition A. For example: pattern 1 (red) consist of a band of 350bp and a small band of 70bp (the PCR product before enzymatic digestion was around 420 bp) after digestion with BstNI and of a band of 380bp and one of 40bp after digestion with CviQI. With L, smart ladder ranging from 200-10000bp; bp, base pairs.

them to be used in the SAS for negative selection and the T1 samples for positive selection. Consequently, the samples could be used for the SAS because nine patients had elevated IgM levels and eight patients had elevated IgG levels at T1. Furthermore, we observed that total IgM plasma levels were significantly increased at 20-33 DPI compared to 1-4 DPI, while IgG levels remained stable. This is in contrast to earlier findings in the literature, a significant increase of total IgG serum levels, but not IgM, was found in

SCI patients one month post-injury (35). However, research in experimental rat models showed that both total IgM and IgG serum levels were decreased after acute cervical SCI (14 DPI), whereas in mice models a SCI at thoracic level was found to increase antibody levels (14 DPI) (15, 36). The level of injury is suggested to play a major role in the antibody synthesis after SCI (36-38). Injury above thoracic level T3 disrupts autonomic control of the spleen, resulting in fewer splenic B cells and impaired antibody

Table 3 – Overview of colony PCR and enzymatic digests with BstNI and CviQI.

Number of colonies		
PCR successes	128	
PCR fails	64	
PCR success rate	66.67%	
Length cDNA insert:		
0-100 bp	51	
100-200 bp	36	
200-300 bp	11	
300-500 bp	20	
500-1000 bp	10	
Fingerprint successes	128	
Fingerprint fails	0	
Recurring patterns:	Condition A	Condition B
1	16	20
2	5	3
3	5	8
4	4	1
5	3	0
Total	33	32
Unique pattern	29	34
Pattern/total ratio	53.23%	48.48%
Unique/total ratio	46.77%	51.52%

Length of the cDNA inserts is estimated based on the bands of the PCR product (on gel) before digestion and after subtracting the size of the empty phage vector (438bp). With PCR, polymerase chain reaction; bp, base pairs.

synthesis (38). Therefore, our results may be partially explained by the fact that we had plasma samples of both cervical and thoracic SCI patients, which could have influenced the antibody levels. However, we did not find any significant differences when comparing thoracic and cervical level injuries. Furthermore, the lack of increase in IgG levels could be due to some early samples in which the IgG responses were not fully activated yet, ten of the T1 SCI samples were collected before 25 DPI (seven on 21 DPI, two on 23 DPI and one on 24 DPI) (13). Another

possible explanation for this result could be the small sample size of our research, we were only able to include 12 SCI patients. Further research is required comparing IgM and IgG levels of a larger SCI patient group to age- and gender-matched healthy controls.

In this research, we optimised the IgM SAS observing the binding capacity and cross-reactivity of anti-human IgM beads. We advanced to an excellent protocol in four subsequent tests, observing the IgM and IgG levels in the samples. In addition, the cross-reactivity was counteracted with a predepletion step to remove IgG antibodies from the plasma samples for the IgM SAS and the other way around for the IgG SAS. Following optimisation, the goal was to perform both the IgM and IgG SAS in parallel and observe the IgM and IgG induction of SCI, however, the IgM SAS will be investigated further in the future.

By performing the IgG SAS, we observed SCI patient’s autoantibody reactivity to phage expressing spinal cord proteins and subsequent selection in four different conditions over the course of four consecutive selection rounds. The ratio input/output was used to observe phage enrichment. Enrichment indicates that specific phage clones have been amplified over the course of the SAS rounds. Each round, phage to which SCI-induced antibodies were reactive to were selected and amplified, increasing the output while keeping the input constant. Furthermore, this reduces the ratio, so enrichment is seen as a reduction in the ratio input/output. During the first round, there did not seem to be any difference in ratios between the different conditions. In the second round, a slight decrease in the ratios of the conditions without IPTG (A and B) was detected compared to the ones with phage produced under the influence of IPTG (C and D). Contrastingly, in the third round, no difference was detected based on IPTG, but the conditions incubated with plasma (A and C) had lower ratios than their negative controls (B and D), as expected. However, the fourth round showed no difference based on IPTG or between plasma and no plasma. In summary, there did not appear to be any clear differences in enrichment between the condition across the four rounds based on output titres and ratios.

As stated previously, IPTG activates the phage’s *Lac* promoter, resulting in increased expression of desired target proteins expressed by the phage (33, 34, 39). However, IPTG was discovered to influence phage production, at

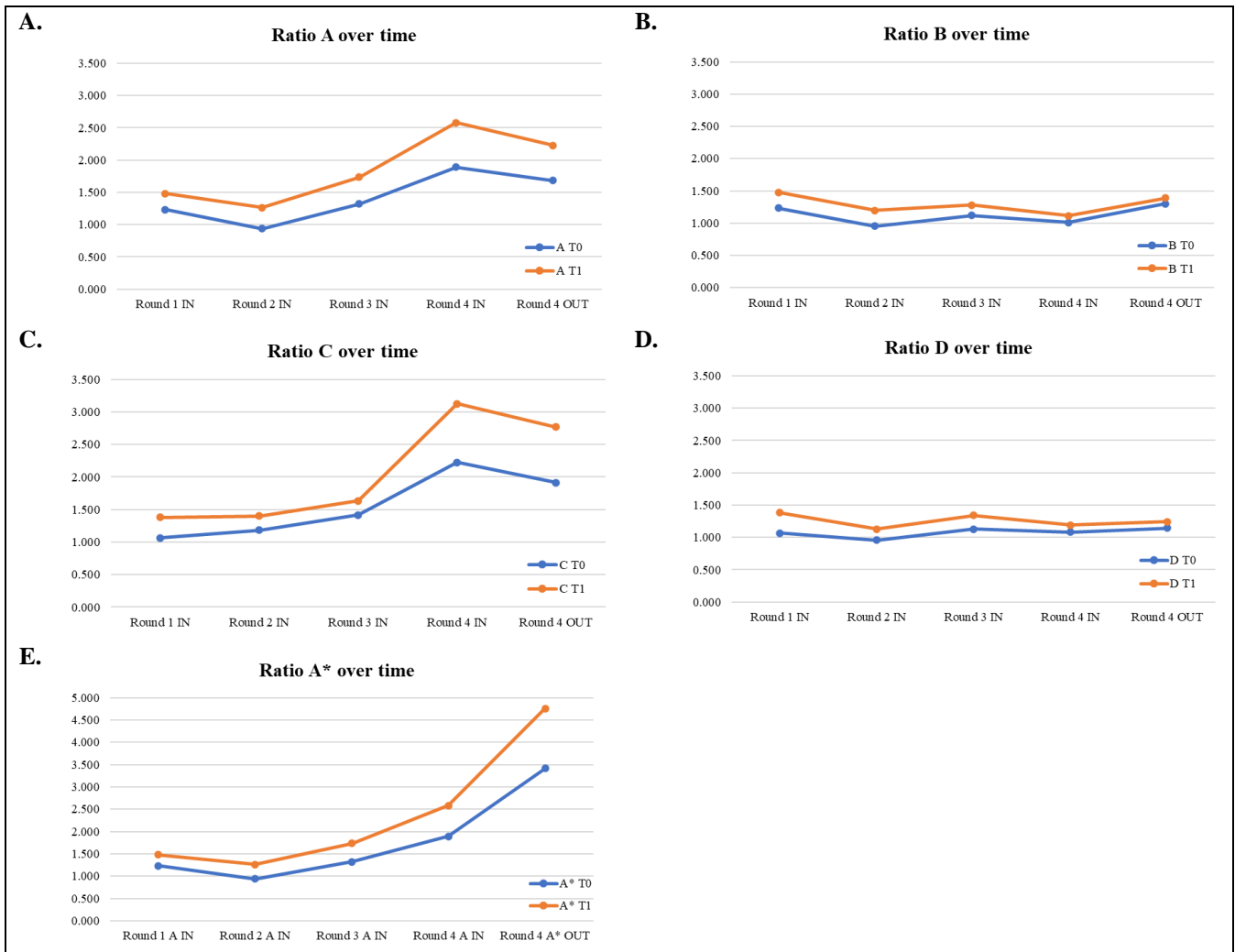


Figure 3 – Reactivity of SCI patients’ samples to phage across four SAS rounds. Phage ELISA was used to determine the reactivity of the T0 and T1 SAS pools to the input and output across four SAS rounds. Optical densities were used as a measure of reactivity. Reactivity to phage of the SAS and to empty phage were measured and the ratio SAS phage/empty phage was calculated and presented in this figure. **A.** The reactivity of T0 and T1 pools for condition A across the four SAS rounds. **B.** for condition B, **C.** for condition C, **D.** for condition D and **E.** for condition A*. With over times, across the four SAS rounds. T0, SCI patients’ plasma samples collected one to four days post injury; T1, 20-33 days post injury. Round 1 IN, the input phage of the spinal cord library, for A, A* and B these are the same, for C and D these phage were produced with IPTG. Round 2 IN, the input for the second round which is the amplified output of the first round. Round 3 IN, the input for the third round of SAS, which is the amplified output of the second round. Round 4 IN, the input for the fourth round, so the amplified output of the third round. Round 4 OUT, the amplified output of the fourth round.

37°C, decreasing phage titres ten to 1000 times compared to a condition without IPTG (40). Another study mentioned phage production after IPTG was reduced three to four fold at 37°C, 30°C and 25°C when compared to phage grown without IPTG (39). However, IPTG improved the efficiency of selection of specific phage, increasing output phage titres at different temperatures four to 20-fold (33, 34, 39). Contrary to expectations, we did not observe any difference in the initial (input) phage titres between conditions grown with or without IPTG. Furthermore, no difference in output titres was

detected after selection, indicating no increased enrichment. A possible explanation may be that these differences become apparent after fingerprinting and sequencing the selected enriched clones of all conditions. Perhaps, proteins identified from clones selected in conditions A and B (without IPTG) may originate more from non-specific and empty phage, whereas clones of conditions C and D (with IPTG) may be more likely to contain true spinal cord injury fusion proteins. But this is to be resolved by sequencing.

Furthermore, contrary to expectations, this study did not find a significant difference in output titres between the conditions with and without plasma. The phage selected by the plasma-free conditions will not express spinal cord proteins but rather antigens specific for reagents used during the SAS enriched during the selection rounds (e.g. milk protein, agarose, ...). However, we also detected this effect in the control A* of A, which was newly introduced in the third and fourth round, in which the plaque was not enriched across four rounds, implying that a large proportion of A's output was also non-specific phage. To counteract this, two negative selections were performed to remove non-specific phage and in the fourth round, a third negative selection was added, however, the non-specific proportion remains substantial.

Interesting was the lack of enrichment across the four rounds, we expected the plasma conditions' ratios to decrease across the four selection rounds, indicating enrichment, but this was not the case. That being said, the DNA fingerprinting and sequencing of all conditions might provide more insights about the enrichment of the conditions.

Fingerprint analyses of 192 randomly selected clones using colony PCR and enzymatic digestion with BstNI and CviQI provided information about the size and digestion products of the phage's cDNA inserts. The insert sizes of the clones ranged from two to 1000 bp, which is consistent with the insert size distribution of the original spinal cord library of 50 to 1300 bp (24). Five patterns were identified in the digestion products of condition A and four patterns in condition B. Four of the five patterns were identified in both the A and B conditions, implying the same phage clones were selected in the condition with and without plasma. This could be explained in part because we only fingerprinted a small proportion of the conditions. The patterns found in both A and B are most likely digestion products of non-specific phage inserts against SAS reagents. Furthermore, the patterns found in A and B may be very similar but not identical, which is difficult to determine with gel electrophoresis but may be resolved by sequencing the phage clones. The percentage of patterned colonies in the A condition is slightly higher than in the B condition, indicating that the plasma condition is more enriched than its plasma-free control. Future DNA fingerprinting and sequence of all conditions, will be very interesting to further elaborate and observe the

enrichment and the effect of IPTG on fusion protein expression in SAS.

The phage ELISA was performed to test SCI autoantibody reactivity against phage of the in- and output samples from each SAS round for each condition to determine phage enrichment. The phage ELISA reported increased reactivity of the T0 and T1 pools towards the phage of the SAS, after four rounds for the A and C conditions. Moreover, the reactivity towards conditions A and C was distinctly higher than their negative controls B and D, except for A*. The increased reactivity across the four rounds of SAS suggests enrichment of specific phage in the SAS, implying that specific phage clones were selected by SCI-induced autoantibodies from the plasma and amplified during SAS, resulting in a large number of copies. In the first round, antibodies will be able to react to only a few copies of a specific phage, but after selection and amplification, there will be more copies to respond to, resulting in higher reactivity. Consequently, the increased reactivity across the SAS can be interpreted as an enrichment of specific phage selected by SCI-induced autoantibodies. The lack of enrichment in conditions B and D is due to the fact that they were not incubated with plasma, and thus phage were selected based on non-specific characteristics, resulting in non-specific phage plaque. The seemingly paradoxical strong A* reactivity could be due to a sample mix-up in the SAS or a phage ELISA error. The slight decrease in reactivity in the fourth round for conditions A and C might be explained by the enrichment being maximised in the third SAS round.

Additionally, the reactivity of the antibodies in the T1 pool towards the phage selected in the SAS was higher than the T0 pool. The lower T0 reactivity was attributable to the fact that phage selected by antibodies from T0 plasma were removed during the negative selection. However, the T0 sample's reactivity was still unexpectedly high, implying that the negative selection did not work optimally. Moreover, because the T0 and T1 samples were obtained from the same patients, a large portion of the antibodies were most likely present in both the T0 and T1 samples.

Surprisingly, the data from the titres calculated following the SAS and the phage ELISA differ. The SAS titres indicate no to very little enrichment, whereas the phage ELISA shows increased reactivity over the consecutive SAS rounds. This inconsistency of lower SAS output titres could be due to inaccurate dilution or

an uncountable number of colonies on certain titration plates. Since the phage ELISA reveals such high reactivity, which increases through the four rounds, we strongly consider there is enrichment and that phage clones were selected by SCI-induced autoantibodies. Additionally, the DNA fingerprinting data confirms this conclusion.

Further research should be conducted to fingerprint all the selected clones of the other conditions and sequence those clones. In addition, performing the IgM SAS to compare IgM and IgG responses to specific spinal cord proteins will provide insights into the humoral responses following SCI. Correlating these SCI-induced autoantibodies with the SCI course could result in biomarkers with prognostic value.

CONCLUSION

In summary, we developed an in-house IgM ELISA and SAS, which provided us with high-quality, optimised techniques. Consequently, exploring the antibody reactivity profile after SCI in 12 SCI patients using a human spinal cord cDNA phage display library and IgG SAS, which provided us with around ten million selected phage. The SAS data in combination with the reactivity profile of the antibodies revealed enrichment of phage selected by SCI-induced autoantibodies. The SAS output was used to randomly select 2016 colonies, of which 192 were DNA fingerprinted, identifying five enriched patterns. Further future characterisation of the selected phage clones will provide more insight into the role of the humoral immune component within SCI. Furthermore, correlation of SCI patients' autoantibodies could potentially provide prognostic strategies.

REFERENCES

1. Sezer N, Akkus S, Ugurlu FG. Chronic complications of spinal cord injury. *World J Orthop.* 2015;6(1):24-33.
2. Craig A, Tran Y, Middleton J. Psychological morbidity and spinal cord injury: a systematic review. *Spinal Cord.* 2009;47(2):108-14.
3. Wang Y, Xie H, Zhao X. Psychological morbidities and positive psychological outcomes in people with traumatic spinal cord injury in Mainland China. *Spinal Cord.* 2018;56(7):704-11.
4. Spinal cord injury [Internet]. 2013. Available from: <https://www.who.int/news-room/fact-sheets/detail/spinal-cord-injury>.
5. Freund P, Seif M, Weiskopf N, Friston K, Fehlings MG, Thompson AJ, et al. MRI in traumatic spinal cord injury: from clinical assessment to neuroimaging biomarkers. *Lancet Neurol.* 2019;18(12):1123-35.
6. Schaefer DM, Flanders AE, Osterholm JL, Northrup BE. Prognostic significance of magnetic resonance imaging in the acute phase of cervical spine injury. *J Neurosurg.* 1992;76(2):218-23.
7. Marino RJ, Graves DE. Metric properties of the ASIA motor score: subscales improve correlation with functional activities. *Arch Phys Med Rehabil.* 2004;85(11):1804-10.
8. Ahuja CS, Fehlings M. Concise Review: Bridging the Gap: Novel Neuroregenerative and Neuroprotective Strategies in Spinal Cord Injury. *Stem Cells Transl Med.* 2016;5(7):914-24.
9. Cristante AF, Barros Filho TE, Marcon RM, Letaif OB, Rocha ID. Therapeutic approaches for spinal cord injury. *Clinics (Sao Paulo).* 2012;67(10):1219-24.
10. Ydens E, Palmers I, Hendrix S, Somers V. The Next Generation of Biomarker Research in Spinal Cord Injury. *Mol Neurobiol.* 2017;54(2):1482-99.
11. Karman J, Ling C, Sandor M, Fabry Z. Initiation of immune responses in brain is promoted by local dendritic cells. *J Immunol.* 2004;173(4):2353-61.
12. Mizrachi Y, Ohry A, Aviel A, Rozin R, Brooks ME, Schwartz M. Systemic humoral factors participating in the course of spinal cord injury. *Paraplegia.* 1983;21(5):287-93.
13. Skoda D, Kranda K, Bojar M, Glosova L, Baurle J, Kenney J, et al. Antibody formation against beta-tubulin class III in response to brain trauma. *Brain Res Bull.* 2006;68(4):213-6.
14. Ankeny DP, Guan Z, Popovich PG. B cells produce pathogenic antibodies and impair recovery after spinal cord injury in mice. *J Clin Invest.* 2009;119(10):2990-9.
15. Ankeny DP, Lucin KM, Sanders VM, McLaughly VM, Popovich PG. Spinal cord injury triggers systemic autoimmunity: evidence for chronic B lymphocyte activation and lupus-like autoantibody synthesis. *J Neurochem.* 2006;99(4):1073-87.
16. Hayes KC, Hull TC, Delaney GA, Potter PJ, Sequeira KA, Campbell K, et al. Elevated serum titres of proinflammatory cytokines and CNS autoantibodies in patients with chronic spinal cord injury. *J Neurotrauma.* 2002;19(6):753-61.
17. Clynes R, Maizes JS, Guinamard R, Ono M, Takai T, Ravetch JV. Modulation of immune complex-induced inflammation in vivo by the coordinate expression of activation and inhibitory Fc receptors. *J Exp Med.* 1999;189(1):179-85.
18. Wada N, Shimizu T, Shimizu N, de Groat WC, Kanai AJ, Tyagi P, et al. The effect of neutralization of nerve growth factor (NGF) on bladder and urethral dysfunction in mice with spinal cord injury. *NeuroUrol Urodyn.* 2018;37(6):1889-96.
19. Abdul-Majid KB, Stefferl A, Bourquin C, Lassmann H, Linington C, Olsson T, et al. Fc receptors are critical for autoimmune inflammatory damage to the central nervous system in experimental autoimmune encephalomyelitis. *Scand J Immunol.* 2002;55(1):70-81.
20. Griot-Wenk M, Griot C, Pfister H, Vandeveld M. Antibody-dependent cellular cytotoxicity (ADCC) in antimyelin antibody-induced oligodendrocyte damage in vitro. *Schweiz Arch Neurol Psychiatr (1985).* 1991;142(2):122-3.
21. Narang A, Qiao F, Atkinson C, Zhu H, Yang X, Kulik L, et al. Natural IgM antibodies that bind neopeptides exposed as a result of spinal cord injury, drive secondary injury by activating complement. *J Neuroinflammation.* 2017;14(1):120.
22. Linington C, Morgan BP, Scolding NJ, Wilkins P, Piddlesden S, Compston DA. The role of complement in the pathogenesis of experimental allergic encephalomyelitis. *Brain.* 1989;112 (Pt 4):895-911.

23. Jazayeri SB, Beygi S, Shokraneh F, Hagen EM, Rahimi-Movaghar V. Incidence of traumatic spinal cord injury worldwide: a systematic review. *Eur Spine J.* 2015;24(5):905-18.
24. Palmers I, Ydens E, Put E, Depreitere B, Bongers-Janssen H, Pickkers P, et al. Antibody profiling identifies novel antigenic targets in spinal cord injury patients. *J Neuroinflammation.* 2016;13(1):243.
25. Govarts C, Somers K, Hupperts R, Stinissen P, Somers V. Exploring cDNA phage display for autoantibody profiling in the serum of multiple sclerosis patients: optimization of the selection procedure. *Ann N Y Acad Sci.* 2007;1109:372-84.
26. Somers K, Stinissen P, Somers V. Optimization of high-throughput autoantibody profiling for the discovery of novel antigenic targets in rheumatoid arthritis. *Ann N Y Acad Sci.* 2009;1173:92-102.
27. Kuhle J, Gaiottino J, Leppert D, Petzold A, Bestwick JP, Malaspina A, et al. Serum neurofilament light chain is a biomarker of human spinal cord injury severity and outcome. *J Neurol Neurosurg Psychiatry.* 2015;86(3):273-9.
28. Ahadi R, Khodagholfi F, Daneshi A, Vafaei A, Mafi AA, Jorjani M. Diagnostic Value of Serum Levels of GFAP, pNF-H, and NSE Compared With Clinical Findings in Severity Assessment of Human Traumatic Spinal Cord Injury. *Spine (Phila Pa 1976).* 2015;40(14):E823-30.
29. Kwon BK, Streijger F, Fallah N, Noonan VK, Belanger LM, Ritchie L, et al. Cerebrospinal Fluid Biomarkers To Stratify Injury Severity and Predict Outcome in Human Traumatic Spinal Cord Injury. *J Neurotrauma.* 2017;34(3):567-80.
30. Zajarias-Fainsod D, Carrillo-Ruiz J, Mestre H, Grijalva I, Madrazo I, Ibarra A. Autoreactivity against myelin basic protein in patients with chronic paraplegia. *Eur Spine J.* 2012;21(5):964-70.
31. Albayar AA, Roche A, Swiatkowski P, Antar S, Ouda N, Emara E, et al. Biomarkers in Spinal Cord Injury: Prognostic Insights and Future Potentials. *Front Neurol.* 2019;10:27.
32. Somers V, Govarts C, Hellings N, Hupperts R, Stinissen P. Profiling the autoantibody repertoire by serological antigen selection. *J Autoimmun.* 2005;25(3):223-8.
33. Intasai N, Arooncharus P, Kasinrerak W, Tayapiwatana C. Construction of high-density display of CD147 ectodomain on VCSM13 phage via gpVIII: effects of temperature, IPTG, and helper phage infection-period. *Protein Expr Purif.* 2003;32(2):323-31.
34. Wang L, Radic MZ, Siegel D, Chang T, Bracy J, Galili U. Cloning of anti-Gal Fabs from combinatorial phage display libraries: structural analysis and comparison of Fab expression in pComb3H and pComb8 phage. *Mol Immunol.* 1997;34(8-9):609-18.
35. Arevalo-Martin A, Grassner L, Garcia-Ovejero D, Paniagua-Torija B, Barroso-Garcia G, Arandilla AG, et al. Elevated Autoantibodies in Subacute Human Spinal Cord Injury Are Naturally Occurring Antibodies. *Front Immunol.* 2018;9:2365.
36. Uldreaj A, Tzekou A, Mothe AJ, Siddiqui AM, Dragas R, Tator CH, et al. Characterization of the Antibody Response after Cervical Spinal Cord Injury. *J Neurotrauma.* 2017;34(6):1209-26.
37. Oropallo MA, Held KS, Goenka R, Ahmad SA, O'Neill PJ, Steward O, et al. Chronic spinal cord injury impairs primary antibody responses but spares existing humoral immunity in mice. *J Immunol.* 2012;188(11):5257-66.
38. Lucin KM, Sanders VM, Jones TB, Malarkey WB, Popovich PG. Impaired antibody synthesis after spinal cord injury is level dependent and is due to sympathetic nervous system dysregulation. *Exp Neurol.* 2007;207(1):75-84.
39. Chappel JA, He M, Kang AS. Modulation of antibody display on M13 filamentous phage. *J Immunol Methods.* 1998;221(1-2):25-34.
40. Kuba H, Furukawa K. An optimized procedure for efficient phage display of antibody fragments with a low folding efficiency. *Protein Expr Purif.* 2009;65(2):148-53.

Acknowledgements – I want to thank Astrid Pues and dr. Judith Fraussen for the supervision and helpful feedback. Additionally, I want to thank the participants of the neuromeeting: professor Veerle Somers, dr Judith Fraussen and dr. Patrick Vandormael. Furthermore, I am thankful for Igna Rutten who helped me with technical lab information. Lastly, I want to thank the SCI patients and HC who donated samples and the institutions where the samples were collected. I want to thank UBiLim for the sample collection.

Author contributions – Astrid Pues gave me guidance and daily supervision. I did most of the data collection, analyses and interpretation with help from my supervisor. I did the writing of the paper after which I received feedback from Astrid Pues and dr. Judith Fraussen.

SUPPLEMENTALS

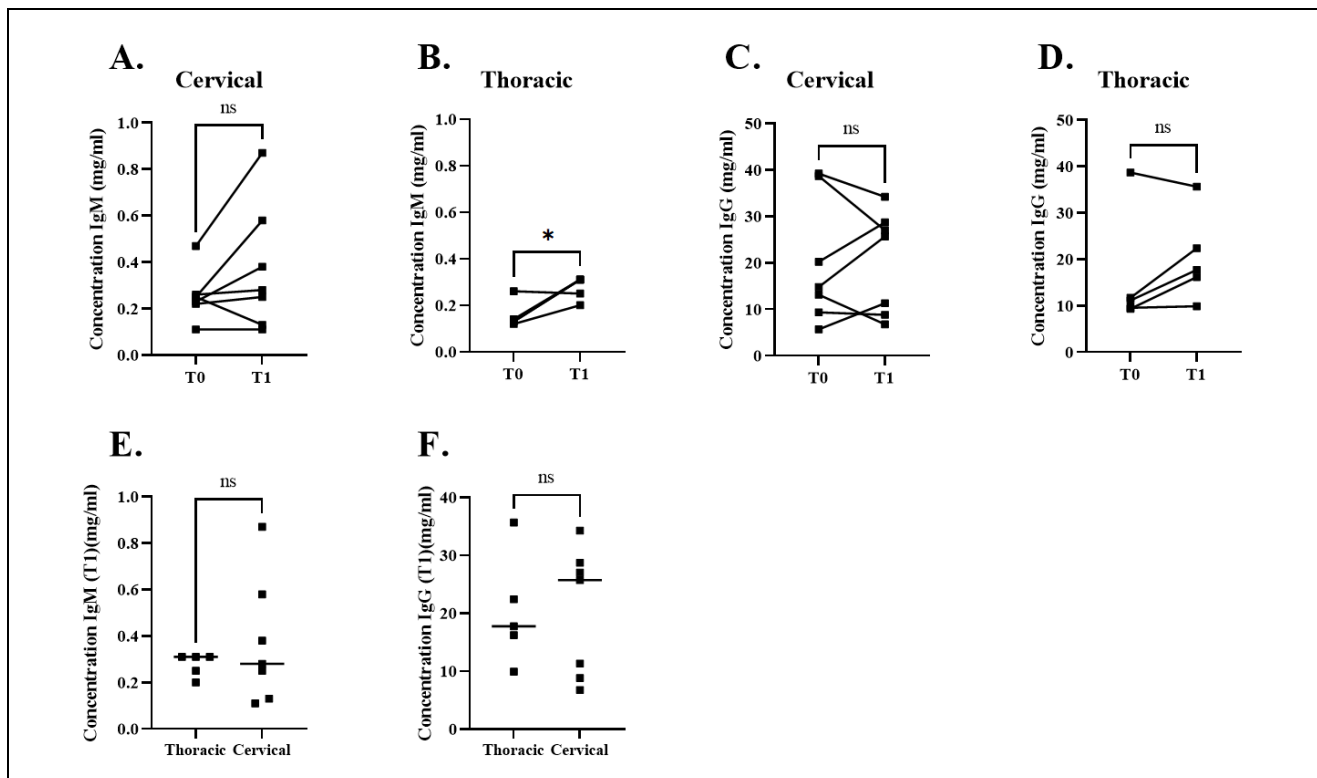
Supplemental methods:

IgM and IgG enzyme-linked immunosorbent assays – To assess the samples' suitability for the SAS, total IgM and IgG concentrations were determined in the T0 (0-4 DPI) and T1 (20-33 DPI) patient samples using IgM and IgG enzyme-linked immunosorbent assays (ELISA). Ninety-six well plates (Greiner Bio-one, Wemmel, Belgium, 391-3610) were coated overnight at 4°C with either 1µg/ml rabbit anti-human IgM (Agilent, Leuven, Belgium, A0425) or 10µg/ml rabbit anti-human IgG (Agilent, Leuven, Belgium, A0423), diluted in coating buffer (0.1M carbonate, 0.03M Na₂CO₃ and 0.07M NaHCO₃). The excess antibodies were washed away in two wash steps using 0.05% PBS-T. The plates were then blocked using 2% dried milk powder (Marvel, London, England) in PBS (2% MPBS) for two hours at 37°C while shaking. After blocking, the plates were washed twice with 0.05% PBS-T. A standard curve (human IgM standard [Jackson, Zottegem, Belgium, 009000012, range 0-100 ng/ml] or human IgG isotype control [Invitrogen, Geel, Belgium, 02-7102, range 0-100 ng/ml]) and plasma samples (diluted 1/10000, 1/30000, 1/90000 and 1/270000 for IgM and 1/500000, 1/1000000 and 1/2000000 for IgG in 2% MPBS) were added to the wells in duplicate and incubated for two hours at RT while shaking. Subsequently, the plates were washed four times, followed by incubation with a rabbit anti-human IgM horseradish peroxidase (HRP, Sigma-Aldrich, Overijse, Belgium, A0420) or rabbit anti-human IgG-HRP (Agilent, Leuven, Belgium, P0214) detection antibody diluted in 2% MPBS (1/50000 and 1/2000 respectively) for one hour, at RT while shaking. After four additional wash steps, 3,3',5,5'-tetramethylbenzidine (TMB, Sigma-Aldrich, Overijse, Belgium, T2885-5G) was added and incubated, ten minutes for IgM and four minutes for IgG ELISA, in the dark. The colour reaction was stopped with 2N H₂SO₄ (VWR, Leuven, Belgium, 1102.2500), and the OD was measured at 450nm with a Tecan Freedom evo plate reader

(Tecan, Männedorf, Switzerland). Based on the standard curve obtained through the standard dilutions, the IgM and IgG concentrations were calculated.

Phage ELISA – To observe enrichment across the SAS rounds, phage ELISA was performed to measure the reactivity of the T0 and T1 pools towards the SAS phage in- and outputs of each selection round. Ninety-six well plates were coated with 2µg/ml mouse monoclonal antibody to M13 phage coat proteins (Sino Biological Huissen, The Netherlands, 11973-MM05T) diluted in coating buffer overnight at 4°C. The plates were washed twice with 0.1% PBS-T and once with 1x PBS for 5 minutes. The wells were then blocked with 5% MPBS and incubated for two hours at 37°C while shaking. After which the plates were washed thrice with 0.1% PBS-T and once with 1x PBS. Next the plates were incubated with the diluted empty phage (diluted in 5% MPBS to 7x10¹¹ cfu) and specific phage (diluted in 5% MPBS to 7x10¹¹ cfu) for one hour at 37°C under static conditions followed by a 30 minutes incubation at RT while shaking. After washing, the diluted T0 and T1 pools (1/20 in 5% MPBS) were incubated for one hour at 37°C under static conditions followed by 30 min incubation at RT while shaking. Washing steps were repeated, and the diluted secondary antibody HRP-labeled goat anti-human IgG-Fc (1/10000 in 5% MPBS, Bethyl laboratories, Montgomery, USA, A80-304P-6) was added for one hour at RT while shaking. TMB was added after washing and incubated in the dark for fifteen minutes. The colour reaction was stopped using 2N H₂SO₄. OD was measured with the Tecan plate reader at 450nm. To determine if the antibody reactivity was directed against the specific antigen and not against phage coat proteins the ratio $\frac{\text{OD specific phage}}{\text{OD empty phage}}$ should be above 1.2.

Supplementary figure:



Supplementary figure 1 – Differences in plasma IgM and IgG concentration between thoracic and cervical level of injury. Measured with IgM and IgG ELISA. **A.** IgM plasma concentration of cervical level SCI patients at T0 and T1. **B.** IgM plasma concentration of thoracic level SCI patients at T0 and T1. **C.** IgG plasma concentration of cervical level SCI patients at T0 and T1. **D.** IgG plasma concentration of thoracic level SCI patients at T0 and T1. **E.** IgM levels at T1 in cervical and thoracic level SCI patients. **F.** IgG levels at T1 in cervical and thoracic level SCI patients. With SCI, spinal cord injury; ns, not significant; T0, first sample collected one to four days post injury; T1, second sample collected 20-33 days post injury. All data were compared with the non-parametric Mann-Whitney test ($n_{cervical}=7$ and $n_{thoracic}=5$) * $p<0.05$.

Supplementary tables:

Supplementary table 1 – Summary of HC characteristics included in this study.

	Age	Gender		IgM level pool (mg/ml)	IgG level pool (mg/ml)
HC	37.6 ± 13.8 years	Male 7 (46.7%)	Female 8 (53.3%)	12.21	429.03

HC were not age or gender matched to the SCI patients. These HC were selected to create a plasma pool with high IgM and IgG levels. The HC were only used to optimise techniques. Data are presented as mean ± standard deviation, number of HC with percentage or total level. With HC, healthy controls; IgM, immunoglobulin M; IgG, immunoglobulin G. ($n_{HC}=15$)

Supplementary table 2 – Testing the binding capacity of the IgM beads.

	Input (%)	T0 (%)	T10 (%)	T30 (%)	T60 (%)	E1 (%)	E2 (%)
Test 1	0.00		57.75	84.24	97.42	11.91	0.00
Test 2	0.00	36.98	54.31	73.33	76.34	0.00	0.56
Test 3	0.00	29.08	59.67	86.86	92.78	20.10	

Data are presented as percentage IgM bound to the IgM selection beads, by measuring the concentration of IgM in the supernatant with IgM ELISA. Pooled plasma of 15 HC was used. Test 1 was a preliminary test in which the IgM selection beads were incubated with the plasma. Test 2 was performed after depleting the sample of IgG using IgG selection beads, the IgM was first eluted with glycine and then with TEA. Test 3 was first depleted of IgG and then eluted only using TEA. The IgM measured in the supernatant before incubation was observed as 100% in the supernatant or 0% bound to the beads. The percentages IgM of the incubations were calculated based on the input. The elutions (E1 and E2) are the percentage IgM in the supernatant calculated based on the percentage IgM on the IgM beads after 60 minutes. With T0, percentage IgM bound to the beads 0 minutes after incubation of the pooled plasma with the beads; T10, 10 minutes after incubation; T30, 30 minutes after incubation; T60, 60 minutes after incubation; E1, percentage IgM in the supernatant after elution with TEA and E2, after elution with glycine; HC, healthy controls; TEA, triethylamine. (n_{HC}=15)

Supplementary table 3 – Testing the cross-reactivity of the IgM beads.

	Input (%)	T0 (%)	T10 (%)	T30 (%)	T60 (%)	E1 (%)	E2 (%)
Test 1	0.00		17.21	20.13	20.00	<0.00	<0.00
Test 2	0.00	<0.00	<0.00	<0.00	<0.00	<0.00	0.25
Test 3	0.00	<0.00	<0.00	<0.00	<0.00	<0.00	

Data are presented as percentage IgG bound to the IgM selection beads, by measuring the concentration of IgG in the supernatant with IgG ELISA. Pooled plasma of 15 HC was used. Test 1 was a preliminary test in which the IgM selection beads were incubated with the plasma. Test 2 was performed after depleting the sample of IgG using IgG selection beads, the IgG was first eluted with glycine and then with TEA. Test 3 was first depleted of IgG and then eluted using only TEA. The IgG measured in the supernatant before incubation was observed as 100% in the supernatant or 0% bound to the beads. The percentages IgM of the incubations were calculated based on the input. The elutions are the percentage IgM in the supernatant calculated based on the percentage IgM on the IgM beads after 60 minutes. With T0, percentage IgG bound to the beads 0 minutes after incubation of the pooled plasma with the beads; T10, 10 minutes after incubation; T30, 30 minutes after incubation; T60, 60 minutes after incubation; E1, percentage IgG in the supernatant after elution with TEA and E2, after elution with glycine; HC, healthy controls; TEA, triethylamine. (n_{HC}=15)

Supplementary table 4 – Overview of the selection process of enriched phage on SCI plasma.

Condition	Round 1	Ratio I/O	Round 2	Ratio I/O	Round 3	Ratio I/O	Round 4	Ratio I/O	
A	Input 1 -	2.35 x 10 ¹³		4.15 x 10 ¹²		3.52 x 10 ¹³		4.80 x 10 ¹³	
	Input 2 -			2.27 x 10 ¹²		3.62 x 10 ¹³		6.20 x 10 ¹²	
	Input 3 +	6.50 x 10 ¹²		4.01 x 10 ¹²		4.88 x 10 ¹³		5.66 x 10 ¹²	
	Input 4 -							5.05 x 10 ⁵	
	Output 1	1.60 x 10 ⁷	4.08 x 10 ⁵	6.20 x 10 ⁶	6.47 x 10 ⁵	8.75 x 10 ⁷	5.58 x 10 ⁵	1.56 x 10 ⁶	3.62 x 10 ⁶
	Output 2	1.08 x 10 ⁷	6.05 x 10 ⁵	1.92 x 10 ⁶	2.08 x 10 ⁶	3.65 x 10 ⁷	1.34x 10 ⁶	6.00 x 10 ⁵	9.44 x 10 ⁶
	Output 3							6.76 x 10 ⁴	7.47 x 10 ⁰
A*	Input 1 -					3.52 x 10 ¹³		4.80 x 10 ¹³	
	Input 2 -					4.10 x 10 ¹³		1.67 x 10 ¹³	
	Input 3 +					3.86 x 10 ¹³		1.71 x 10 ¹³	
	Input 4 -							2.19 x 10 ⁶	
	Output 1					7.30 x 10 ⁷	5.29 x 10 ⁵	4.93 x 10 ⁷	3.46 x 10 ⁵
	Output 2					1.44 x 10 ⁶	2.69 x 10 ⁷	2.66 x 10 ⁶	6.42 x 10 ⁶
	Output 3							1.40 x 10 ⁵	1.57 x 10 ¹
B	Input 1 -	1.13 x 10 ¹³		1.07 x 10 ¹³		5.80 x 10 ¹³		2.32 x 10 ¹³	
	Input 2 -			2.32 x 10 ¹³		4.70 x 10 ¹³		1.79 x 10 ¹³	
	Input 3 +	2.65 x 10 ¹²		2.15 x 10 ¹³		4.28 x 10 ¹³		3.15 x 10 ¹³	
	Input 4 -							9.23 x 10 ⁵	
	Output 1	1.11 x 10 ⁷	2.40 x 10 ⁵	5.05 x 10 ⁶	4.25 x 10 ⁶	4.85 x 10 ⁷	8.83 x 10 ⁵	4.74 x 10 ⁶	6.65 x 10 ⁶
	Output 2	1.47 x 10 ⁷	1.81 x 10 ⁵	2.00 x 10 ⁶	1.07 x 10 ⁷	2.11 x 10 ⁶	2.03 x 10 ⁷	5.60 x 10 ⁶	5.63 x 10 ⁶
	Output 3							1.43 x 10 ⁵	6.44 x 10 ⁰
C	Input 1 -	1.76 x 10 ¹³		9.70 x 10 ¹³		5.54 x 10 ¹³		1.94 x 10 ¹³	
	Input 2 -			6.20 x 10 ¹³		3.16 x 10 ¹³		4.91 x 10 ¹²	
	Input 3 +	2.80 x 10 ¹²		1.34 x 10 ¹³		1.13 x 10 ¹³		6.43 x 10 ¹²	
	Output 1	1.10 x 10 ⁷	2.54 x 10 ⁵	5.45 x 10 ⁶	2.46 x 10 ⁶	8.11 x 10 ⁷	1.39 x 10 ⁵	3.68 x 10 ⁷	1.75 x 10 ⁵
	Output 2	1.61 x 10 ⁷	1.74 x 10 ⁵	1.43 x 10 ⁶	9.39 x 10 ⁶	3.28 x 10 ⁷	3.44 x 10 ⁵	1.78 x 10 ⁶	3.61 x 10 ⁶
	Output 3								
	D	Input 1 -	1.56 x 10 ¹³		6.40 x 10 ¹²		3.00 x 10 ¹³		3.57 x 10 ¹³
Input 2 -				1.60 x 10 ¹³		3.26 x 10 ¹³		9.75 x 10 ¹²	
Input 3 +		6.15 x 10 ¹²		5.60 x 10 ¹³		3.52 x 10 ¹³		7.03 x 10 ¹²	
Output 1		1.05 x 10 ⁷	5.89 x 10 ⁵	2.34 x 10 ⁶	2.39 x 10 ⁷	3.66 x 10 ⁷	9.61 x 10 ⁵	3.42 x 10 ⁶	2.05 x 10 ⁶
Output 2		2.39 x 10 ⁷	2.58 x 10 ⁵	6.73 x 10 ⁵	8.32 x 10 ⁷	1.14 x 10 ⁷	3.09 x 10 ⁶	1.01 x 10 ⁶	6.94 x 10 ⁶
Output 3									

Supplementary table 4 – Overview of the selection process of enriched phage on SCI plasma.

Titration of phage in the input and output samples of SAS presented as colony forming unit/ml. In condition **A** pooled SCI patients' plasma was incubated with the library, **B** was a negative control of **A** incubated without plasma. **A*** was an additional negative selection of condition **A** starting from the same input as **A** in round **3** and **4**. For condition **C** phage of the spinal cord library were produced with isopropyl thio-b-D-galactopyranoside (IPTG) and incubated with SCI plasma, whereas **D** was a negative control of **C** with no plasma. Input 1 was the input for the first negative selection, in the first round this is the human spinal cord library, in the second round this is the output of the first round, for the third round the output of the second round, and so on for the following rounds. Input 2 is the supernatant of the first negative selection and the input for the second negative selection, input 3 is the supernatant of the second negative selection and the input of the positive selection. The first output is after elution with TEA, the second output after elution with glycine. For the fourth round of SAS an additional negative selection was added on the precipitated eluate of the positive selection, this was only done for condition **A**, **A*** and **B**. The third output is the supernatant after the additional negative selection. The ratios are calculated by dividing the third input by the outputs, and for the fourth round this is the fourth input divided by the third output. Across the four rounds, the ratio input to output phage titres provides a measurement of enrichment of phage clones. The higher the output, the lower the ratio input/output, and thus more enrichment. With Ratio I/O, ratio between the input and the outputs. ($n_{\text{SCI patients}}=12$)